Contribution from the Department of Chemistry and Laboratory for Molecular Structure and Bonding, Texas A&M University, College Station, Texas 77843

Dinuclear Niobium(IV) Complexes $Nb_2Cl_4(OMe)_4L_2$ (L = MeOH, CH_3CN) and Their Relation to Analogous W and Mo Compounds

F. Albert Cotton,* Michael P. Diebold, and Wieslaw J. Roth

Received April 2, 1987

A dinuclear Nb(IV) complex of the formula $Nb_2Cl_4(OMe)_4(MeOH)_2 \cdot 2MeOH$ (**1**) is conveniently prepared by dissolution of $NbCl_4(CH_3CN)_3$ in methanol. This compound crystallizes in monoclinic space group $P2_1/n$ with a = 9.231 (2) Å, b = 8.961 (2) Å, c = 13.236 (1) Å, β = 91.75 (1)°, V = 1094.4 (6) Å^3, and Z = 2. Recrystallization of **1** from acetonitrile affords $Nb_2Cl_4(OMe)_4(CH_3CN)_2$ (**2**), which has a different disposition of terminal ligands. It crystallizes in the triclinic system ($P\bar{1}$) with a = 9.716 (4) Å, b = 15.439 (5) Å, c = 6.663 (2) Å, α = 91.39 (2)°, β = 98.70 (3)°, γ = 102.89 (3)°, V = 961 (1) Å^3, and Z = 2. The difference between the solid-state structures of **1** and **2**, together with the proton NMR spectrum of the former, indicates that axial and equatorial terminal ligands interchange easily. The molecular structure and bonding in the Nb complexes are compared to those in related W and Mo species of the formula $M_2X_4(OR)_4L_2$, where L = ROH and RO^-.

Introduction

The isolation of a dinuclear Nb(IV) complex of the formula $Nb_2Cl_4(OMe)_4(MeOH)_2 \cdot 2MeOH$ (**1**), which we reported in a preliminary communication,[1] was considered of special interest since related tungsten complexes have been known and thoroughly investigated.[2] However, the synthetic method affording the Nb compound was hardly a convenient one, and alternative methods have been sought. It was found that a compound of identical stoichiometry had been prepared by reacting $NbCl_4 \cdot 3CH_3CN$ with methanol[3] but it had been formulated as a monomeric octahedral $NbCl_2(OMe)_2(MeOH)_2$. The unit cell determination for this material proved that it was identical with the dimer, thus making available an efficient method for the preparation of **1**. In this paper we present a full report on crystallographic and spectroscopic characterization of this compound and of its acetonitrile derivative $Nb_2Cl_4(OMe)_4(MeCN)_2$ (**2**).

Experimental Section

All operations were carried out under an atmosphere of argon. Standard vacuum-line techniques were used. $Nb_2Cl_6(THT)_3$,[4] $NbCl_4(CH_3CN)_3$,[5] and $NbCl_4(THF)_2$[5] were prepared according to literature methods. Methanol and acetonitrile were freshly distilled under nitrogen from MgO and P_2O_5, respectively, before use. NMR and IR spectra were recorded on a Varian XL 200 spectrometer and Perkin-Elmer 783 IR spectrometer, respectively.

Reaction of $Nb_2Cl_6(THT)_3$ with MeOH. The dimeric Nb(III) complex (0.38 g, 0.58 mmol) was dissolved in 15 mL of toluene and cooled in an ice bath, and 0.3 mL of MeOH was added. The opaque purple solution was then stored at 5 °C, and its color changed to transparent red within several hours. Microcrystalline red-brown material was also formed (apparently $Nb_2Cl_5(OMe)(MeOH)_4$), and a blue oil deposited at the bottom. The former disappeared, and the latter turned into dark blue crystals of $Nb_2Cl_4(OMe)_4(MeOH)_4$ (**1**) within several days. Yield: approximately 85 mg, 25%.

Preparation of 1 from the $NbCl_4$ Adducts. $NbCl_4(CH_3CN)_3$ or $NbCl_4(THF)_2$ (13.0 mmol) was dissolved in 30.0 mL of MeOH, affording a blue-purple solution after a short time. The volume was then halved under vacuum and the solution placed at −20 °C for 2 days. Crystalline material was isolated by filtration and washed with small amounts of cold MeOH. Yields varied but were consistently above 50%. IR (bands not coincidental with Nujol peaks), cm^{-1}: 300 (s), 455 (w), 488 (m), 512 (s), 590 (s), 830 (w, br), 990 (m), 1005 (s), 1030 (s), 1120 (s, br), 2960 (s), 3250 (m, br), 3400 (s).

Other alcohols (EtOH, *i*-PrOH) also gave blue-purple solutions with UV–visible spectra similar to that of the methoxide derivative, but the products converted to intractable red oils upon workup.

Reaction of 1 with CH_3CN. $Nb_2Cl_4(OMe)_4(MeOH)_4$ (0.5 g, 0.86 mmol) was dissolved in 3 mL of acetonitrile. The solution was stored undisturbed, and transparent purple crystals of $Nb_2Cl_4(OMe)_4(MeCN)_2$ (**2**) were deposited within 1 day (0.18 g, 40%). The solid was isolated by filtration and the solution evaporated to dryness. The residue was treated with 3 mL of acetonitrile, which dissolved only part of the solid. Subsequent filtration afforded an additional crop of **2** (0.15 g) in the form of a brown-purple powder.

IR (bands not coincidental with Nujol peaks), cm^{-1}: 2319 (s), 2295 (s), 1417 (w), 1369 (m), 1153 (m, sh), 1110 (s, br), 1048 (s), 1029 (s), 1015 (w, sh), 973 (w, sh), 948 (w, sh), 830 (w, br), 586 (s), 525 (m), 497 (s), 455 (w), 428 (w), 412 (w), 350 (s), 309 (w, sh).

X-ray Crystallography. General procedures used for data collection and refinement of the structures have been described previously.[6,7]

Table I. Summary of Crystallographic Data

	1	**2**
formula	$Nb_2Cl_4O_8C_8H_{28}$	$Nb_2Cl_4O_4N_2C_8H_{18}$
fw	579.93	533.87
space group	$P2_1/n$	$P\bar{1}$
syst abs	$0k0$, $k \neq 2n$; $h0l$, $h + l \neq 2n$	
a, Å	9.231 (2)	9.716 (4)
b, Å	8.961 (2)	15.439 (5)
c, Å	13.236 (1)	6.663 (2)
α, deg	90.0	91.39 (2)
β, deg	91.75 (1)	98.70 (3)
γ, deg	90.0	102.89 (3)
V, Å^3	1094.4 (6)	961 (1)
Z	2	2
d_{calcd}, g/cm^3	1.760	1.844
cryst size, mm	0.3 × 0.2 × 0.15	0.2 × 0.05 × 0.05
μ(Mo Kα), cm^{-1}	15.209	17.123
data collcn instrum	CAD-4	$P\bar{1}$
radiation (monochromated in incident beam)	Mo Kα (λ_α = 0.71073 Å)	Mo Kα (λ_α = 0.71073 Å)
orientation reflcns: no.; range, deg	25; 16.1 < 2θ < 30.9	15; 13.4 < 2θ < 28.4
temp, °C	22	5
scan method	ω-2θ	ω-2θ
data collcn range (2θ), deg	4–50	4–45
no. of unique data; total with $F_o^2 > 3\sigma(F_o^2)$	1542; 1290	1632; 1140
no. of params refined	100	141
R[a]	0.033	0.045
R_w[b]	0.044	0.057
quality-of-fit indicator[c]	1.181	1.118
largest shift/esd, final cycle	0.15	0.0
largest peak, e/Å^3	0.53	0.66

[a] $R = \sum||F_o| - |F_c||/\sum|F_o|$. [b] $R_w = [\sum w(|F_o| - |F_c|)^2/\sum w|F_o|^2]^{1/2}$; $w = 1/\sigma^2(|F_o|)$. [c] Quality of fit = $[\sum w(|F_o| - |F_c|)^2/(N_{observn} - N_{params})]^{1/2}$.

(1) Cotton, F. A.; Diebold, M. P.; Roth, W. J. *Inorg. Chem.* **1985**, *24*, 3509.
(2) (a) Anderson, L. B.; Cotton, F. A.; DeMarco, D.; Fang, A.; Ilsley, W. H.; Kolthammer, B. W. S.; Walton, R. A. *J. Am. Chem. Soc.* **1981**, *103*, 5078. (b) Cotton, F. A.; Falvello, L. R.; Fredrich, M. F.; DeMarco, D.; Walton, R. A. *J. Am. Chem. Soc.* **1983**, *105*, 3088. (c) Seifert, H. J.; Petersen, F.; Wohrmann, H. *J. Inorg. Nucl. Chem.* **1973**, *35*, 2735.
(3) Gut, R.; Perron, W. *J. Less-Common Met.* **1972**, *26*, 369.
(4) Cotton, F. A.; Duraj, S. A.; Falvello, L. R.; Roth, W. J. *Inorg. Chem.* **1985**, *24*, 4389.
(5) Manzer, L. *Inorg. Chem.* **1977**, *3*, 525.
(6) Crystal structure determinations were carried out by standard methods, which have been described previously: (a) Bino, A.; Cotton, F. A.; Fanwick, P. E. *Inorg. Chem.* **1979**, *18*, 3558. (b) Cotton, F. A.; Frenz, B. A.; Deganello, G.; Shaver, A. *J. Organomet. Chem.* **1973**, *50*, 227.
(7) Calculations were done on the VAX-11/780 computer at the Department of Chemistry, Texas A&M University, College Station, TX, with the VAX-SDP software package.
(8) Cotton, F. A.; DeMarco, D.; Kolthammer, B. W. S.; Walton, R. A. *Inorg. Chem.* **1981**, *20*, 3048.

0020-1669/87/1326-3319$01.50/0

Table II. Positional and Isotropic Equivalent Displacement Parameters for $Nb_2Cl_4(OMe)_4(MeOH)_4$ (**1**)

atom	*x*	*y*	*z*	*B*,[a] Å^2
Nb	0.11733 (5)	0.09433 (6)	0.01893 (3)	2.786 (8)
Cl(1)	0.3262 (2)	0.0827 (2)	0.1357 (1)	5.03 (4)
Cl(2)	0.2443 (2)	0.2803 (2)	−0.0833 (1)	5.23 (4)
O(1)	−0.0305 (4)	0.0778 (4)	−0.0989 (3)	3.06 (7)
O(2)	0.0296 (4)	0.2421 (4)	0.0876 (3)	3.84 (8)
O(3)	0.2440 (4)	−0.0645 (5)	−0.0618 (3)	3.98 (9)
O(4)	0.4187 (5)	−0.2616 (6)	0.0073 (5)	7.5 (1)
C(1)	−0.0610 (7)	0.1524 (9)	−0.1921 (5)	5.3 (2)
C(2)	0.010 (1)	0.3812 (8)	0.1372 (7)	8.0 (2)
C(3)	0.2595 (7)	−0.0822 (9)	−0.1689 (5)	5.6 (2)
C(4)	0.382 (1)	−0.364 (1)	0.0809 (9)	8.6 (3)
H(3)	0.3320	−0.0820	−0.0429	4*
H(4)	0.5273	−0.2226	0.0410	4*
H(11)	−0.1406	0.1406	−0.2089	4*
H(12)	0.0273	0.1679	−0.2304	4*
H(13)	−0.0820	0.2500	−0.1875	4*
H(21)	−0.0566	0.3886	0.0820	4*
H(22)	0.0820	0.4160	0.1250	4*
H(23)	−0.0292	0.3046	0.2070	4*
H(31)	0.1660	−0.1093	−0.1875	4*
H(32)	0.3320	−0.1386	−0.1679	4*
H(33)	0.3320	0.0000	−0.1875	4*
H(41)	0.3046	−0.4179	0.0410	4*
H(42)	0.4707	−0.4179	0.1035	4*
H(43)	0.3906	−0.2792	0.1464	4*

[a] Values marked with an asterisk denote isotropically refined atoms. Values for anisotropically refined atoms are given in the form of the isotropic equivalent thermal parameter defined as $^4/_3[a^2\beta_{11} + b^2\beta_{22} + c^2\beta_{33} + ab(\cos\gamma)\beta_{12} + ac(\cos\beta)\beta_{13} + bc(\cos\alpha)\beta_{23}]$.

Table III. Positional and Isotropic Displacement Parameters for $Nb_2Cl_4(OMe)_4(MeCN)_2$ (**2**)

atom	*x*	*y*	*z*	*B*,[a] Å^2
Nb(1)	0.1087 (2)	−0.20370 (9)	0.1084 (2)	2.15 (3)
Nb(2)	−0.1504 (2)	−0.32739 (9)	0.0381 (2)	2.14 (3)
Cl(1)	0.3232 (5)	−0.1763 (3)	0.3739 (7)	3.5 (1)
Cl(2)	0.0407 (5)	−0.0846 (3)	0.2819 (7)	3.5 (1)
Cl(3)	−0.2655 (4)	−0.4573 (3)	0.2144 (7)	3.4 (1)
Cl(4)	−0.2995 (4)	−0.2474 (3)	0.1897 (7)	3.5 (1)
O(1)	−0.073 (1)	−0.2136 (6)	−0.098 (1)	2.2 (2)
O(2)	0.008 (1)	−0.2945 (6)	0.282 (1)	2.7 (3)
O(3)	0.2018 (9)	−0.2689 (6)	−0.030 (1)	2.3 (2)
O(4)	−0.0882 (9)	−0.4078 (6)	−0.111 (1)	2.3 (2)
N(1)	0.209 (1)	−0.0942 (9)	−0.075 (2)	3.5 (3)
N(2)	−0.331 (1)	−0.3508 (8)	−0.218 (2)	3.5 (3)
C(1)	−0.136 (2)	−0.152 (1)	−0.223 (2)	2.9 (3)*
C(2)	0.026 (2)	−0.309 (1)	0.502 (3)	4.5 (4)*
C(3)	0.330 (2)	−0.286 (1)	−0.095 (3)	3.8 (4)*
C(4)	−0.109 (2)	−0.492 (1)	−0.220 (2)	3.0 (4)*
C(5)	0.261 (2)	−0.043 (1)	−0.178 (3)	3.7 (4)*
C(6)	0.325 (2)	0.024 (1)	−0.311 (3)	4.4 (4)*
C(7)	−0.422 (2)	−0.3651 (9)	−0.355 (2)	2.4 (3)*
C(8)	−0.538 (2)	−0.383 (1)	−0.538 (3)	3.4 (4)*

[a] See footnote *a* in Table II.

Lorentz and polarization corrections were applied to the intensity data before the structure factors were derived. No correction for absorption was necessary. The relevant crystallographic parameters for **1** and **2** are summarized in Table I.

In each case the position of Nb atoms was derived from a three-dimensional Patterson function, and the remainder of the molecular structure was determined by an alternating series of difference Fourier syntheses and least-squares refinements. For **1** all atoms were assigned anisotropic displacement parameters, and the hydrogen atoms were located in the difference Fourier map. They were included in the refinement but with fixed displacement parameters. In the acetonitrile adduct **2**, the carbon atoms were refined isotropically and no attempt was made to locate H atoms.

Tables of observed and calculated structure factors and anisotropic displacement parameters are available as supplementary material.

(9) Chisholm, M. H.; Kirkpatrick, C. C.; Huffman, J. C. *Inorg. Chem.* **1981**, *20*, 871.

Table IV. Important Bond Distances (Å) and Angles (deg) for $Nb_2Cl_4(OMe)_4(MeOH)_4$ (**1**)[a]

Nb–Nb′	2.781 (1)	Nb–O(1)′	2.048 (3)
Nb–Cl(1)	2.436 (1)	Nb–O(2)	1.811 (4)
Nb–Cl(2)	2.465 (2)	Nb–O(3)	2.147 (4)
Nb–O(1)	2.046 (3)		
Nb′–Nb–Cl(1)	133.25 (5)	Cl(2)–Nb–O(2)	90.5 (1)
Nb′–Nb–Cl(2)	133.83 (4)	Cl(2)–Nb–O(3)	84.2 (1)
Nb′–Nb–O(1)	47.2 (1)	O(1)–Nb–O(1)′	94.4 (1)
Nb′–Nb–O(1)′	47.18 (9)	O(1)–Nb–O(2)	97.9 (2)
Nb′–Nb–O(2)	100.2 (1)	O(1)–Nb–O(3)	86.2 (1)
Nb′–Nb–O(3)	86.6 (1)	O(1)′–Nb–O(2)	95.9 (2)
Cl(1)–Nb–Cl(2)	89.83 (6)	O(1)′–Nb–O(3)	89.2 (2)
Cl(1)–Nb–O(1)	167.7 (1)	O(2)–Nb–O(3)	173.2 (2)
Cl(1)–Nb–O(1)′	87.4 (1)	Nb–O(1)–Nb′	85.6 (1)
Cl(1)–Nb–O(2)	94.0 (1)	Nb–O(1)–C(1)	137.4 (4)
Cl(1)–Nb–O(3)	81.6 (1)	Nb′–O(1)–C(1)	137.0 (4)
Cl(2)–Nb–O(1)	87.0 (1)	Nb–O(2)–C(2)	159.6 (5)
Cl(2)–Nb–O(1)′	173.2 (1)	Nb–O(3)–C(3)	129.5 (4)

[a] Numbers in parentheses are estimated standard deviations in the least significant digits.

Table V. Important Bond Distances (Å) and Angles (deg) for $Nb_2Cl_4(OMe)_4(MeCN)_2$ (**2**)[a]

Nb(1)–Nb(2)	2.768 (2)	Nb(2)–Cl(3)	2.483 (4)
Nb(1)–Cl(1)	2.471 (5)	Nb(2)–Cl(4)	2.413 (4)
Nb(1)–Cl(2)	2.413 (4)	Nb(2)–O(1)	2.043 (9)
Nb(1)–O(1)	2.039 (10)	Nb(2)–O(2)	2.034 (10)
Nb(1)–O(2)	2.016 (10)	Nb(2)–O(4)	1.831 (9)
Nb(1)–O(3)	1.814 (9)	Nb(2)–N(2)	2.215 (15)
Nb(1)–N(1)	2.242 (14)		
Nb(2)–Nb(1)–Cl(1)	135.2 (1)	Nb(1)–Nb(2)–O(1)	47.2 (3)
Nb(2)–Nb(1)–Cl(2)	100.1 (1)	Nb(1)–Nb(2)–O(2)	46.6 (3)
Nb(2)–Nb(1)–O(1)	47.4 (3)	Nb(1)–Nb(2)–O(4)	95.4 (3)
Nb(2)–Nb(1)–O(2)	47.1 (3)	Nb(1)–Nb(2)–N(2)	132.1 (4)
Nb(2)–Nb(1)–O(3)	95.1 (3)	Cl(3)–Nb(2)–Cl(4)	85.9 (2)
Nb(2)–Nb(1)–N(1)	132.4 (3)	Cl(3)–Nb(2)–O(1)	173.6 (3)
Cl(1)–Nb(1)–Cl(2)	86.4 (2)	Cl(3)–Nb(2)–O(2)	89.5 (3)
Cl(1)–Nb(1)–O(1)	173.7 (3)	Cl(3)–Nb(2)–O(4)	86.0 (3)
Cl(1)–Nb(1)–O(2)	88.7 (3)	Cl(3)–Nb(2)–N(2)	92.5 (4)
Cl(1)–Nb(1)–O(3)	86.0 (3)	Cl(4)–Nb(2)–O(1)	87.8 (3)
Cl(1)–Nb(1)–N(1)	92.3 (4)	Cl(4)–Nb(2)–O(2)	92.0 (3)
Cl(2)–Nb(1)–O(1)	87.4 (3)	Cl(4)–Nb(2)–O(4)	163.3 (3)
Cl(2)–Nb(1)–O(2)	91.5 (3)	Cl(4)–Nb(2)–N(2)	82.5 (4)
Cl(2)–Nb(1)–O(3)	164.2 (3)	O(1)–Nb(2)–O(2)	91.9 (4)
Cl(2)–Nb(1)–N(1)	83.5 (4)	O(1)–Nb(2)–O(4)	99.8 (4)
O(1)–Nb(1)–O(2)	92.6 (4)	O(1)–Nb(2)–N(2)	85.6 (5)
O(1)–Nb(1)–O(3)	99.8 (4)	O(2)–Nb(2)–O(4)	102.5 (4)
O(1)–Nb(1)–N(1)	85.9 (4)	O(2)–Nb(2)–N(2)	174.0 (4)
O(2)–Nb(1)–O(3)	102.1 (4)	O(4)–Nb(2)–N(2)	83.3 (5)
O(2)–Nb(1)–N(1)	174.9 (5)	Nb(1)–O(1)–Nb(2)	85.4 (4)
O(3)–Nb(1)–N(1)	83.0 (5)	Nb(1)–O(2)–Nb(2)	86.2 (4)
Nb(1)–Nb(2)–Cl(3)	135.4 (1)	Nb(1)–O(3)–C(3)	152.4 (9)
Nb(1)–Nb(2)–Cl(4)	100.6 (1)	Nb(2)–O(4)–C(4)	152.1 (9)

[a] Numbers in parentheses are estimated standard deviations in the least significant digits.

Results

Solid-State Structures. The positional and isotropic equivalent thermal parameters for **1** and **2** are listed in Tables II and III, respectively. Important interatomic dimensions are compiled in Table IV for **1** and in Table V for **2**. Complete listings of bond distances and angles are included in the supplementary material.

$Nb_2Cl_4(OMe)_4(MeOH)_4$. The unit cell contains discrete dinuclear $Nb_2Cl_4(OMe)_4(MeOH)_2$ species and uncoordinated molecules of solvent. The dimer, shown in Figure 1, resides on a crystallographic inversion center. It has an edge-sharing bioctahedral geometry with four terminal Cl atoms and two bridging methoxide ligands in the equatorial plane. The axial positions are occupied by two pairs of methoxide ions and methanol molecules trans to each other. The averaged values of selected interatomic dimensions are listed in Table VI and will be discussed later. The molecules of solvent present in the lattice are hydrogen bonded to the ligating MeOH via H(3) and to Cl(2) from a

Table VI. Averaged Values of Selected Interatomic Distances (Å) and Angles (deg) in the $M_2Cl_4(\mu\text{-}OR)_2(OR)_2X_2$ Complexes[a]

	$Nb_2Cl_4(OMe)_4(MeOH)_4$ (1)	$Nb_2Cl_4(OMe)_4(MeCN)_2$ (2)	$W_2Cl_4(OMe)_4(MeOH)_2$ (3)	$W_2Cl_4(OEt)_6$ (4)	$Mo_2Cl_4(O\text{-}i\text{-}Pr)_6$ (5)
M–M	2.781 (1)	2.768 (2)	2.481 (1)	2.715 (1)	2.731 (1)
M–Cl (trans OR_b)	2.451 [15]	2.477 [6]	2.385 [4]	2.403 [7]	2.419 [1]
M–Cl (trans OR_t)		2.413 (4)			
M–OR_b (trans Cl)	2.047 [1]	2.041 [2]	2.034 [2]	2.012 [1]	2.016 [2]
M–OR_b (trans X)		2.025 [2]			
M–OR_t	1.811 (4)	1.823 [9]	1.950 (5)	1.824 [4]	1.814 [2]
M–X	2.147 (4)	2.228 [14]	2.036 (6)		
M–O–M	85.5 (1)	85.8 [4]	75.2 (2)	84.9 (2)	85.3 [1]
M–O_b–C	137.2 [2]	135.5 [5]	131 [2]	136.8 [3]	137.3 [9]
M–O_t–C	159.6 (5)	152.3 [2]	131.3 (5)	144.6 [6]	145.1 [5]
M–O_t(H)–C	129.5 (4)		130.1 (5)		
ref	this work	this work	3a	8	9

[a] Numbers in brackets are variances, obtained from the expression $[(\sum\Delta_i^2/n(n-1)]^{1/2}$, where Δ_i is the deviation of the ith value from the arithmetic mean and n is the total number of values averaged.

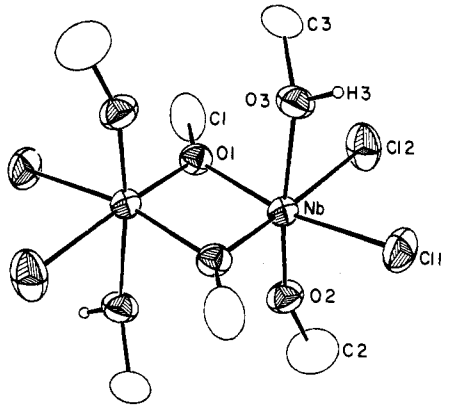

Figure 1. ORTEP drawing of the $Nb_2Cl_4(OMe)_4(MeOH)_2$ (**1**) molecule. The ellipsoids enclose 40% of the electron density. A crystallographic inversion center relates the halves of the molecule.

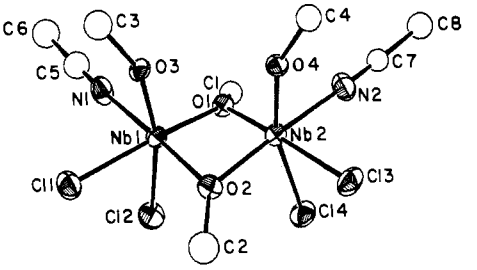

Figure 2. ORTEP drawing of the $Nb_2Cl_4(OMe)_4(MeCN)_2$ (**2**) molecule. The ellipsoids enclose 40% of the electron density.

neighboring molecule via their own hydroxyl proton. The interatomic distances for these hydrogen bonds are O(3)–O(4) = 2.54 Å and Cl(2)–O(4) = 3.25 Å, while the angles O(3)–H(3)–O(4) and Cl(2)–H(4)–O(4) are equal to 129.8 and 147.5°, respectively. The absence of intramolecular hydrogen bonding of the type seen in the W(IV) complex is probably the reason for rather than the result of the intermolecular bonding observed here. In the niobium case the axial oxygen atoms are about 3 Å apart, which precludes the formation of the hydrogen bridge, and the distance is about 0.3 Å longer than the M–M distance. This bending of ligands away from each other is also evident in complex **2** where there is no interference from intermolecular interactions.

$Nb_2Cl_4(OMe)_4(MeCN)_2$. The molecule of complex **2**, which is shown in Figure 2, is located on a general crystallographic position. It has a virtual mirror plane passing through the common edge of the bioctahedron, and the plane is perpendicular to the Nb–Nb axis. Although **2** is formally related to the MeOH adduct only by substitution with the MeCN molecules, it has a completely different disposition of the terminal ligands. There are only two Cl atoms in the equatorial plane, and the other two are now perpendicular to that plane and trans to the methoxide ligands. This rearrangement with respect to **1** results in some changes in bond lengths (see Table VI).

Comparison of the Structures of the $M_2Cl_4(OR)_4X_2$ Complexes. The two niobium compounds reported here provide an opportunity for a direct comparison of structural features and bonding in group 5 and 6 complexes of the general formula $M_2Cl_4(\mu\text{-}OR)_2(OR)_2X_2$, where M = Nb, Mo, and W and X = ROH, MeCN, and RO^-. Table VI lists averaged values of selected bond distances and bond angles for several structurally characterized representatives of this class. All these molecules have an edge-sharing bioctahedral geometry, and except for the doubly metal–metal-bonded W(IV) species, they are isoelectronic and possess a single bond between the metal atoms. While in most cases the bond lengths for the group 6 complexes are shorter than the corresponding ones for Nb, the metal to terminal OR distances fall within a very narrow range and they are very short. The apparent inconsistency for the W(IV) compound is due to internal hydrogen bonding between RO^- and ROH, which tends toward equalization of these two ligands. The short M–O_t distances are due to π donation from oxygen atoms to the metal atoms, as a result of which the bond order becomes greater than 1. The π bonding also results in the opening of the M–O–C angles. The donation appears to be stronger for niobium as evidenced by the closer approach of that angle to linearity; this is consistent with the fact that while the Nb atom is larger than those of Mo and W, the niobium compounds exhibit the same M–O bond length as the latter two.

Solution Properties. $Nb_2Cl_4(OMe)_4(MeOH)_4$ is insoluble in neutral solvents and reacts with some media, e.g. acetone. In coordinating solvents, like acetonitrile, it undergoes substitution leading to mixture of species, and in methanol-d_4, rapid exchange of all methoxide ligands is observed. As a result $CDCl_3$ is essentially the only solvent suitable for the solution study of **1**.

While proton NMR spectra of $W_2Cl_4(OR)_4(ROH)_2$ (R = Et, *i*-Pr) (the methanol derivative was too insoluble for solution studies) in $CDCl_3$ were consistent with the solid-state structures, in the case of niobium methoxide they revealed a complex behavior in solution. At ambient temperatures there is a rapid exchange as evidenced by the broad peaks for methyl protons. Cooling of the solutions gave a series of sharp peaks for the methyl groups, which indicates the presence of well-defined species. The chemical shifts for these signals change only slightly in the temperature range from around −10 to −60 °C (see Figure 3), but their relative intensities vary with temperature and the concentration of free methanol in the medium. The methyl proton resonances appear in three regions, viz. around 5, 4, and 3.5 ppm, due to bridging MeO^-, terminal MeO^-, and MeOH, respectively, and their number indicates that more than one species is present in solution. There are four distinct bridging methoxide peaks, denoted in Figure 3 as a_1, a_2, b, and c, and the following observations were made concerning their intensities:

(a) The relative intensities of peaks a_1 and a_2 remain constant, suggesting that both are associated with one compound containing inequivalent bridges.

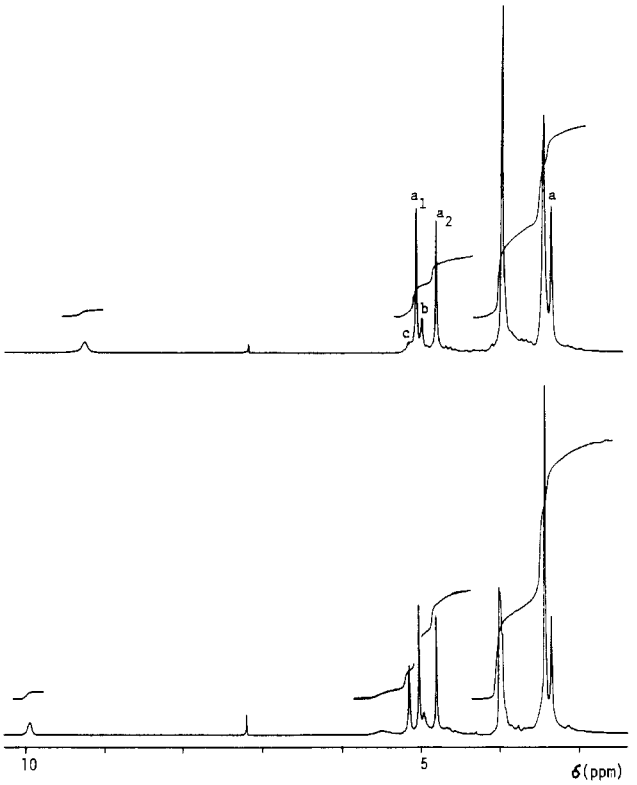

Figure 3. Proton NMR spectrum of **1** in $CDCl_3$ at −10 °C (top) and −60 °C (bottom).

(b) The intensity of peak c increases at the expense of peak b as the temperature is lowered.

(c) The combined intensity of peaks c and b relative to that of peak a_1 (and peak a_2) increases with decreasing temperature and increasing the amount of free MeOH in the medium.

These facts indicate that in solution there is an equilibrium between three dominant molecular species, A, B, and C, dependent upon temperature and concentration of free methanol.

The unresolved signal around 4 ppm encompasses all the terminal MeO resonances. The shoulder on its right-hand side is associated with C and B since it becomes a distinct peak when their concentration is increased by the presence of more free MeOH. While most of the methanol is represented by one signal at 3.45 ppm, a certain fraction is clearly different from the rest as shown by the sharp small peak (a) at 3.35 ppm. It is always of about the same intensity as peaks a_1 and a_2; like them it can be attributed to the A species. Its distinction from the rest of methanol present is probably due to its involvement in hydrogen bonding, most likely an intramolecular one since it is affected by excess MeOH to the same extent as are peaks a_1 and a_2. The corresponding hydroxyl proton signal, clearly seen in the region 9–10 ppm, shifts upfield with increasing temperature or the amount of MeOH, showing that this H atom undergoes slow exchange. This explains the lack of expected HO–CH_3 coupling, and on the basis of arguments put forward by Cotton et al.,[2] the exchange can be attributed to some intermolecular process. The chemical shift for the remaining hydroxyl protons is temperature dependent and varies from 4.5 ppm at −10 °C to 5.5 ppm at −60 °C. It should be noted that the temperture dependence of the spectra is reversible.

The detailed structure of A and, a fortiori, those of B and C must be highly speculative. Species A is required to contain two inequivalent OMe bridges and one strongly attached MeOH molecule with an internally hydrogen-bonded OH proton. B and C most likely contain equivalent bridges and freely exchanging MeOH ligands. Several spatial arrangements of ligands consistent with these requirements are possible. For A, one example is shown in I but structures with other dispositions of ligands might well

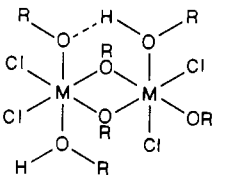

I

be correct. Since there is an inverse relationship between the concentrations of A and MeOH, it may be that A is an oligomer formed due to loss of one MeOH, which would free a coordination site and allow coupling of the dimers. Oligomerization via hydrogen bonding cannot be ruled out either.

The room-temperature spectrum is also quite complex. It is dominated by three broad peaks due to bridging and terminal MeO and MeOH, indicating that there is a mixture of species undergoing rapid exchange. However, there are also several sharp peaks suggesting the presence of small amounts of one or more well-defined species, which do not participate in the exchange and persist even at +55 °C.

The NMR spectrum of **1** in acetonitrile-d_3 indicates almost complete substitution of the ligating methanol molecules and formation of different isomers as shown by the presence of several peaks in each of the regions where bridging and terminal OMe appear. The same situation occurred when solid $Nb_2Cl_4(OMe)_4(CH_3CN)_2$ was repeatedly washed with acetonitrile to remove residual MeOH.

Both the difference between solid-state structures of **1** and **2**, as well as solution behavior show that terminal ligands in $Nb_2Cl_4(OMe)_4L_2$ rearrange readily in contrast to the behavior of the W analogue. In the latter the integrity of the solid-state geometry is preserved by the intramolecular hydrogen bonding between RO^- and ROH groups. Such bonding plays at most a minor role in the Nb complexes, and there is a low-energy barrier for the interconversion of terminal ligands between axial and equatorial positions.

Acknowledgment. We are grateful to the Robert A. Welch Foundation for support. M.P.D. thanks Texaco/IUCCP and the NSF for predoctoral fellowships.

Supplementary Material Available: Proton NMR spectrum of $Nb_2Cl_4(OMe)_4(MeOH)_4$ (**1**) in $CDCl_3$ at room temperature and a complete listing of bond distances, bond angles, and anisotropic thermal parameters for the crystal structures of **1** and **2** (7 pages); tables of observed and calculated structure factors for both structures (13 pages). Ordering information is given on any current masthead page.